Flash graphene induced low-temperature synthesis of a single-crystalline $Na_{2.72}Fe_{1.64}(SO_4)_3$ cathode for boosted sodium storage

Qiming Xiao [a], *Yong Li* [a, b, *], *Kechen Wang* [b], *Canliang Ma* [c], *Bin Liu* [a,*], *Yun Zhao* [b, c, *]

[a] Scientific Instrument Center, Shanxi University, Taiyuan 030006, PR China

[b] Sodium-ion Battery Energy Storage Technology Key Laboratory Cultivation Base Jointly Constructed by the Department and City of Shan Xi Province, Hua Yang Group New Energy Co., Ltd., Yangquan 045000, PR China

[c] Institute of Molecular Science, Shanxi University, Taiyuan 030006, PR China

[*] * Corresponding authors.
E-mail addresses: liyong@sxu.edu.cn (Y. Li); liubin@sxu.edu.cn(B, Liu); zhaoyun@sxu.edu.cn(Y. Zhao).

Material Preparation

The SC-NFS@FG material was prepared via a simple high-energy ball-milling method, followed by an annealing procedure. Flash graphene (FG) was synthesized through the flash Joule heating approach described in the literature using carbon black (Cabot Co.) as a raw material[1]. Initially, $FeSO_4 \cdot 7H_2O$ (99.0 %, Aladdin) was dehydrated in an argon atmosphere in a tube furnace at 250°C for 4 h to produce anhydrous $FeSO_4$. Subsequently, 0.136 mol of Na_2SO_4 (99.0 %, Macklin), 0.164 mol of anhydrous $FeSO_4$, and 2.21 g of FG were accurately weighed and mixed together. The mixture was then ball-milled under an Ar atmosphere for 6 h, resulting in a uniform black powder precursor, which is denoted as P-SC-NFS@FG. Finally, the precursor was annealed at 350°C under an argon atmosphere for 12 h to form the SC-NFS@FG. For comparison, a control sample, PC-NFS, was prepared using the same procedure but omitting the addition of FG. Its milled precursor is denoted as P-PC-NFS. Analogous precursors were also prepared using carbon black (CB) and carbon nanotubes (CNT) in place of FG; these are denoted as P-PC-NFS@CB and P-PC-NFS@CNT, respectively. For comparison, PC-NFS was prepared using the same procedure but omitting the addition of FG. Its precursor after ball-milling is denoted as P-PC-NFS. In addition, comparative precursors were also prepared using carbon black (CB) and carbon nanotubes (CNT) in place of FG; these are denoted as P-PC-NFS@CB and P-PC-NFS@CNT, respectively.

Material Characterizations

The crystal structure was characterized using X-ray diffractometry (XRD, Bruker

D8 Advance). The morphology of the samples was observed using scanning electron microscopy (SEM, JSM-7900F) and transmission electron microscopy (TEM, JEOL JEM-2100Plus). Elemental distribution was detected via energy-dispersive X-ray spectroscopy (EDS) mapping analysis using a spectrometer attached to the TEM. Thermal gravimetric analysis (TGA, Netzsch STA449C) was conducted at a heating rate of 10 ℃/min in a nitrogen atmosphere. N_2 adsorption/desorption isotherms were measured at 77 K with an ASAP 2020 physisorption apparatus. Raman spectroscopy (LabRAM HR Evolution) was employed for structural analysis, while Fourier-transform infrared spectroscopy (FTIR, Thermo Scientific Nicolet iS50) and X-ray photoelectron spectroscopy (XPS, ESCALAB 250Xi) were used to analyze chemical bonds and functional groups, and elemental composition and chemical state, respectively.

Electrochemical Measurement

The performance of the material was evaluated using CR-2025 button cells. The batteries were assembled in an argon-filled glovebox with water and oxygen levels maintained below 0.1 ppm. A slurry was prepared by blending the active material, conductive agent (AB), and polyvinylidene fluoride (PVDF, Arkema-HSV900) in a 7:2:1 mass ratio, with the addition of N-methyl-2-pyrrolidone (NMP, Aladdin). The slurry was then applied onto aluminum foil and vacuum-dried at 110°C for 12 h. Each electrode was loaded with 1.5-2.0 mg cm^{-1} of the material. The negative electrode is sodium metal foil, while a glass fiber (Whatman, GF/D 1823-047mm) acts as the separator. The electrolyte was a 1 mol L^{-1} $NaClO_4$ solution in a mixture of ethylene

carbonate, diethyl carbonate, and fluoroethylene carbonate (EC/DEC, 1:1 v/v, with an additional 5% FEC). Half-cell constant current charge-discharge tests and galvanostatic intermittent titration technique (GITT) were conducted using the LAND CT2001A instrument (Wuhan, China). Electrochemical impedance spectroscopy (EIS) and cyclic voltammetry (CV) measurements were performed using a CHI660E electrochemical workstation (Shanghai Chenhua).

The data processing details of CV tests at various scan rates

According to the relationship (Equations (1) and (2)) between the measured current (i) and the scan rate (v) [2]:

$$i = av^b \tag{1}$$

$$logi = b \times logv + loga \tag{2}$$

Where a and b are adjustable parameters. Notably, when the b-value approaches or exceeds 1, the electrochemical reaction system is predominantly governed by a capacitive process. In contrast, when the b-value is approximately 0.5, the insertion/de-insertion process for Na^+ ions is primarily controlled by diffusion. The over-all pseudocapacitance contribution from 2.0-4.5 V can be calculated according to Equation (3):

$$i(V) = k_1 v + k_2 v^{0.5} \tag{3}$$

Where v is the sweep rate, and V is the fixed potential. By determining both parameters k_1 and k_2, it is thus possible to determine the capacitive contribution to the total current at different states of charge and discharge[3].

The calculation details of Na^+ diffusion coefficients based on EIS results

The Na^+ diffusion coefficients were calculated as follows:

$$D_{Na+} = \frac{R^2T^2}{2A^2n^4F^4C^2\sigma^2} \quad (4)$$

where R, T, A, n, F, C and σ represent gas constant, temperature, surface area, the number of electrons transferred in the reaction process, Faraday constant, concentration of Na^+ and Warburg constant, respectively[4,5].

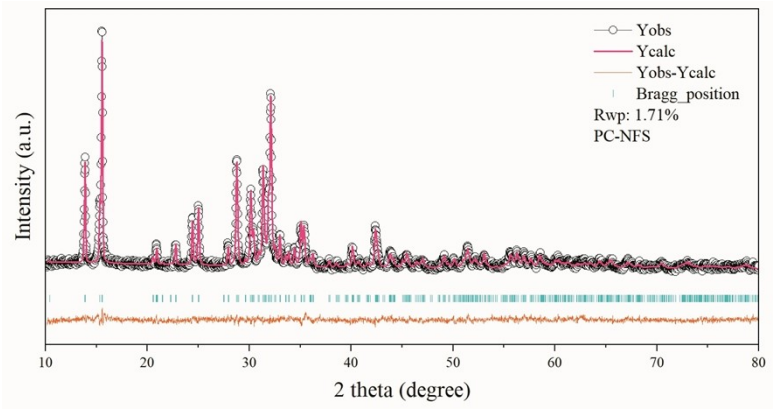

Fig S1. The XRD pattern and Rietveld refinement of PC-NFS.

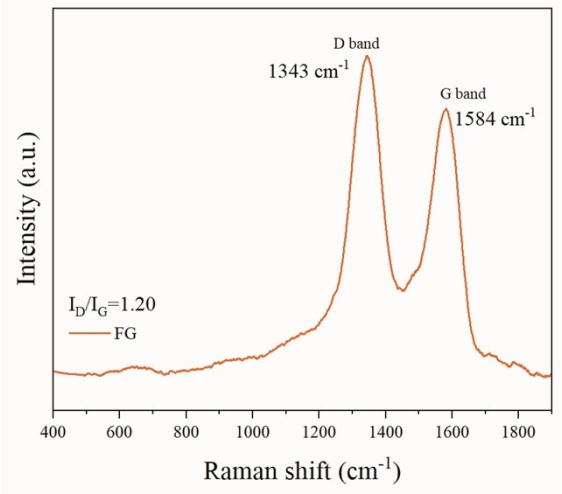

Fig S2. Raman spectra of pure FG.

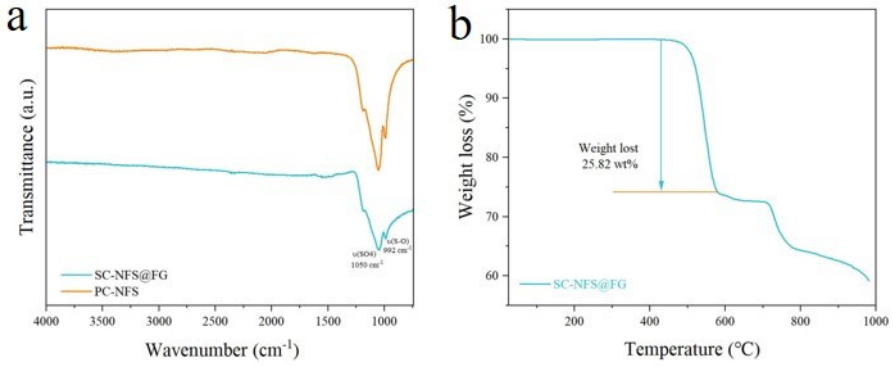

Fig S3. (a) FT-IR spectra of SC-NFS@FG and PC-NFS. (b) The TGA curve of SC-NFS@FG.

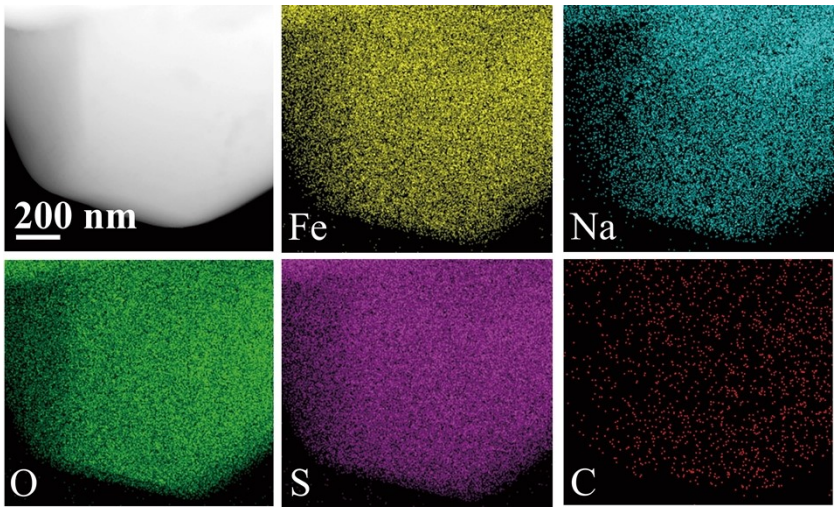

Fig S4. The elemental mapping results of HRTEM-EDS for the SC-NFS@FG sample.

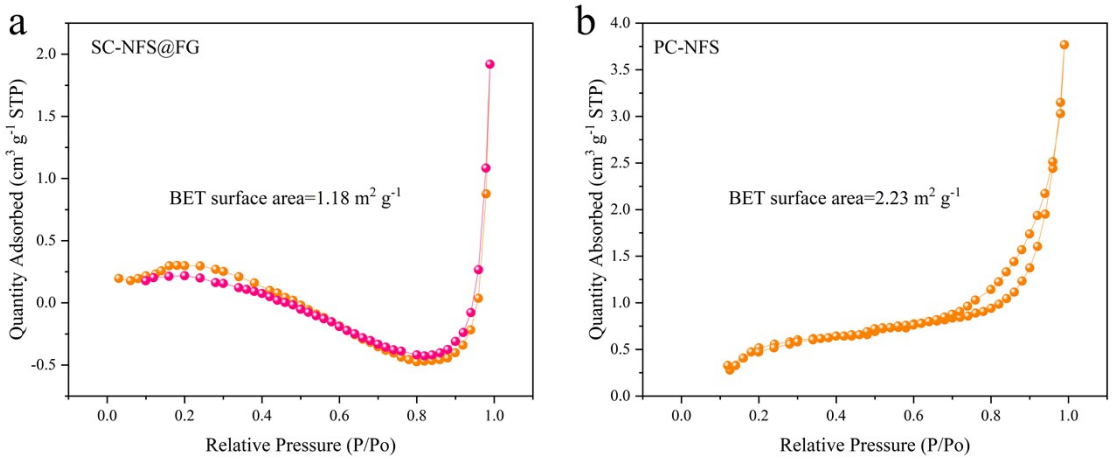

Fig S5. N_2 adsorption/desorption isotherms. (a) SC-NFS@FG, (b) PC-NFS.

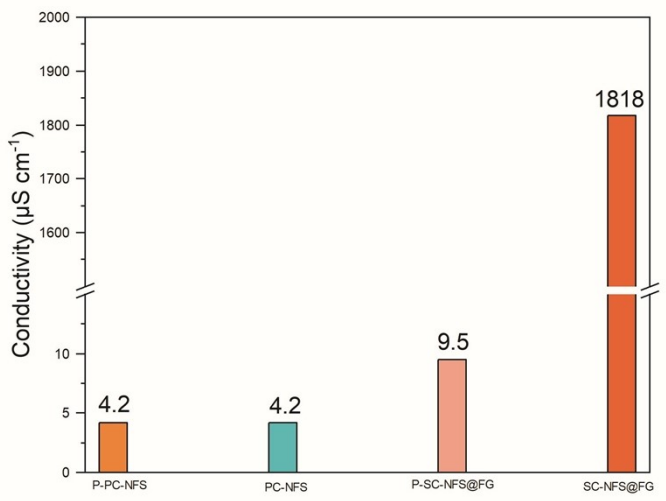

Fig S6. Electrical conductivity comparison of P-PC-NFS, PC-NFS, P-SC-NFS@FG and SC-NFS@FG.

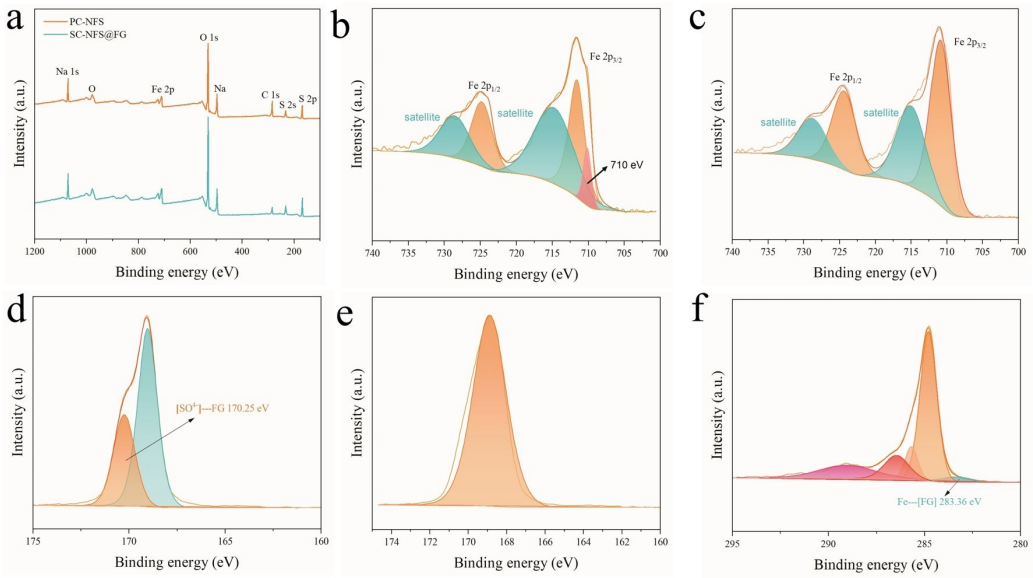

Fig S7. XPS survey spectra of SC-NFS@FG and PC-NFS (a). Fe 2p XPS spectra of SC-NFS@FG (b) and PC-NFS (c). S 2p XPS spectra of SC-NFS@FG (d) and PC-NFS (e). C 1s XPS spectrum of SC-NFS@FG (f).

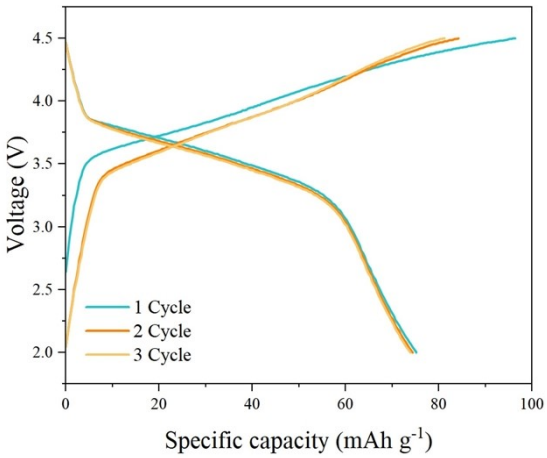

Fig S8. The charge-discharge profiles of the first three cycles of the PC-NFS cathode at 0.1C.

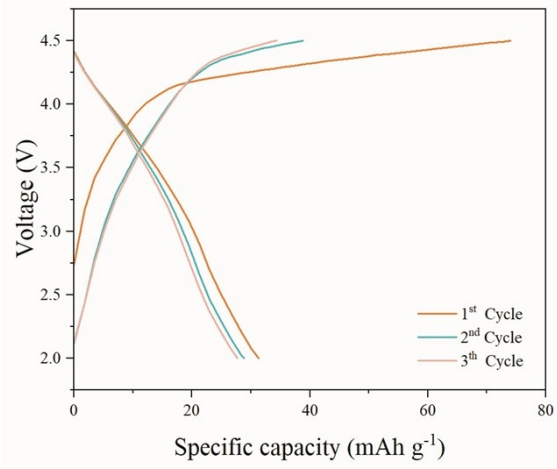

Fig S9. Corresponding charge/discharge curves of the first three cycles of FG as the cathode for sodium-ion batteries at 0.1 C in a voltage range of 2.0-4.5 V vs. Na/Na^+.

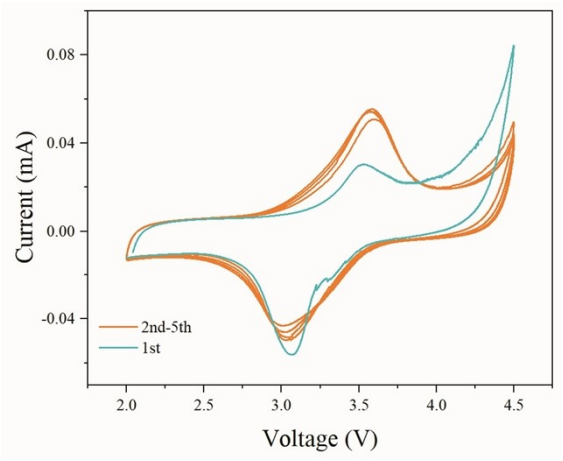

Fig S10. The cyclic voltammetry curves of PC-NFS at 0.25 mV s^{-1}.

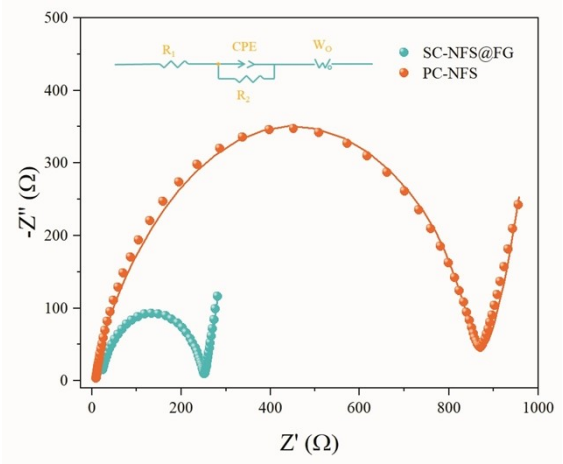

Fig S11. EIS spectra of the SC- NFS@FG and PC-NFS electrode.

Note: the Nyquist plots are fitted by the Zview software and the results are summarized in Table S3.

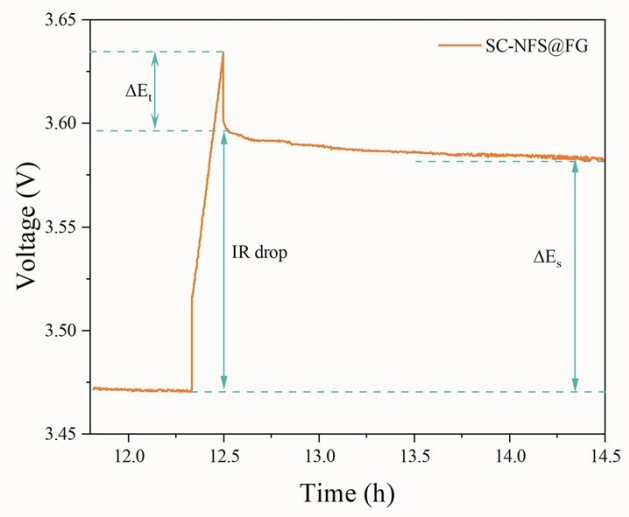

Fig S12. Enlarged GITT curve of the SC-NFS@FG electrode.

The equation for D_{Na^+} is as follows:

$$D_{Na^+} = 4L^2/\pi\tau \left(\frac{\Delta E_s}{\Delta E_\tau}\right)^2 \quad (\tau \leq L^2/D_{Na^+}) \qquad \text{(S1)}$$

Where L is the effective thickness of the electrode material, τ is the pulse time, π is 3.14, ΔE_s is the open circuit potential difference between two adjacent pulse, and ΔE_τ is the change of potential caused by an impulse.

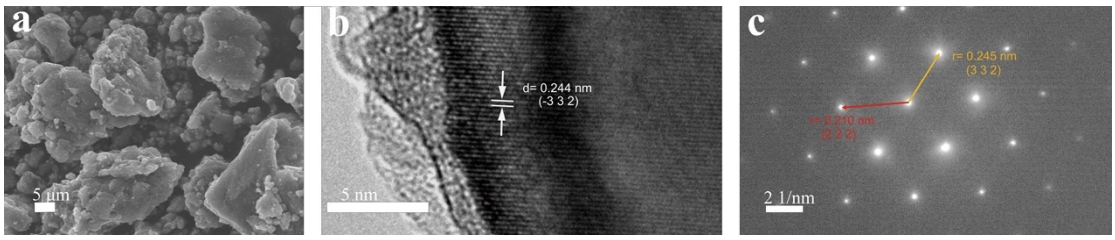

Fig S13. (a) SEM image, (b) HRTEM image and (c) SAED pattern of cycled SC-NFS@FG electrodes after 3000 cycles at 15 C.

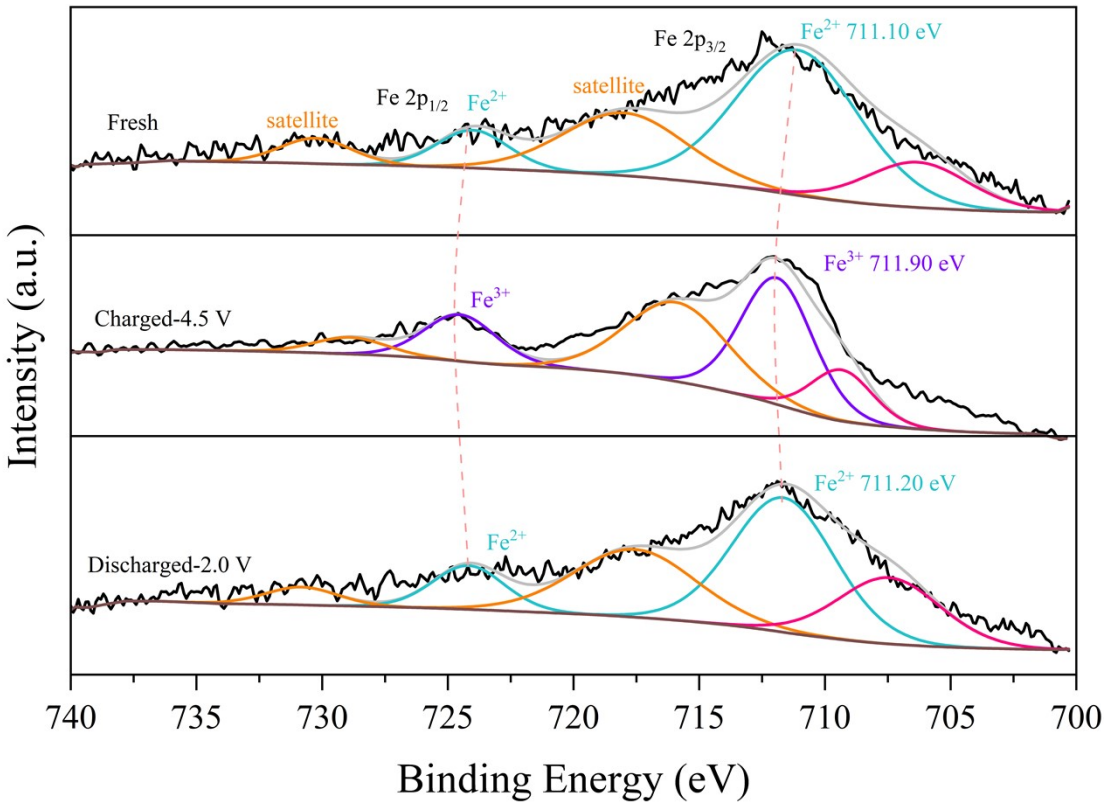

Fig S14. Fe 2p XPS spectra recorded at different potentials.

Table S1. Crystallographic information of SC-NFS@FG after the Rietveld refinement.

Formula	$Na_{2.72}Fe_{1.64}(SO_4)_3$@FG
Crystal system	Monoclinic
Space group	C 2/c
a (Å)	12.64676
b (Å)	12.77682
c (Å)	6.51559
Unit cell volume ($Å^3$)	949.835
α	90
β	115.54414
γ	90
Source	XRD
Wave length (Å)	1.54056
2θ range	10-80°
Rwp (%)	1.52

Atom	*x*	*y*	*z*	Occ
Na1	0.50000	0.73224	0.75000	0.375
Na2	0.00000	0.00000	0.00000	0.488
Na3	0.50000	0.99250	0.25000	0.488
Fe1	0.73148	0.15708	0.14876	1.000
S1	0.00000	0.77299	0.75000	0.900
S2	0.76627	0.60316	0.87533	0.100
O1	0.08506	0.84599	0.71565	1.000
O2	0.45406	0.20699	0.54887	1.000
O3	0.76751	0.67072	0.69175	1.000
O4	0.31973	0.99282	0.37362	1.000
O5	0.35428	0.59269	0.65187	1.000
O6	0.33187	0.17159	0.09579	1.000

Table S2. Crystallographic information of PC-NFS after the Rietveld refinement.

Formula	$Na_{2.72}Fe_{1.64}(SO_4)_3$			
Crystal system	Monoclinic			
Space group	C 2/c			
a (Å)	12.64680			
b (Å)	12.77049			
c (Å)	6.51718			
Unit cell volume ($Å^3$)	949.672			
α	90			
β	115.54499			
γ	90			
Source	XRD			
Wave length (Å)	1.54056			
2θ range	10-80°			
Rwp (%)	1.69			
Atom	*x*	*y*	*z*	Occ
Na1	0.50000	0.73034	0.75000	0.375
Na2	0.00000	0.00000	0.00000	0.488
Na3	0.50000	0.98964	0.25000	0.488
Fe1	0.73161	0.15835	0.15001	1.000
S1	0.00000	0.77438	0.75000	0.900
S2	0.76674	0.60214	0.87753	0.100
O1	0.08839	0.84537	0.72366	1.000
O2	0.45325	0.20822	0.55008	1.000
O3	0.76775	0.66956	0.68918	1.000
O4	0.32320	0.99323	0.38115	1.000
O5	0.35337	0.59578	0.65848	1.000
O6	0.33200	0.17210	0.08915	1.000

Table S3. Equivalent circuit fitting parameters of EIS plots

Samples	R_1	R_2	Zw
SC-NFS@FG	20.43	231	0.42
PC-NFS	9.06	857.1	0.39

Note: the determined values of the physical elements R_1 representing electrolyte impedance, CPE symbolizing constant phase element, R_2 associated with charge transfer impedance pertaining to the Faraday process, and Wo denoting Warburg impedance[6].

References

1 M. G. Stanford, K. V. Bets, D. X. Luong, P. A. Advincula, W. Chen, J. T. Li, Z. Wang, E. A. McHugh, W. A. Algozeeb, B. I. Yakobson and J. M. Tour, *ACS Nano*, 2020, **14**, 13691–13699.

2 X. Pu, D. Zhao, C. Fu, Z. Chen, S. Cao, C. Wang and Y. Cao, *Angew. Chem. Int. Ed.*, 2021, **60**, 21310–21318.

3 M. Chen, D. Cortie, Z. Hu, H. Jin, S. Wang, Q. Gu, W. Hua, E. Wang, W. Lai, L. Chen, S. Chou, X. Wang and S. Dou, *Adv. Energy Mater.*, 2018, **8**, 1800944.

4 Z. Zhao, Y. Zou, P. Liu, Z. Lai, L. Wen and Y. Jin, *Electrochimica Acta*, 2022, **418**, 140350.

5 X. Wang, H. Hao, J. Liu, T. Huang and A. Yu, *Electrochimica Acta*, 2011, **56**, 4065–4069.

6 G. Yao, X. Zhang, Y. Yan, J. Zhang, K. Song, J. Shi, L. Mi, J. Zheng, X. Feng and W. Chen, *J. Energy Chem.*, 2020, **50**, 387–394.